Friction Modeling in Dynamic Robot Simulation *

Pierre E. Dupont

Robotics Laboratory
Harvard University, Cambridge, MA 02138

Abstract

This paper discusses the importance of appropriately modeling friction for the simulation and control of high performance robot systems. Incorporating Coulomb-type friction in the dynamic equations introduces two difficulties in the forward dynamic solution. We show that the differential equations become discontinuous in the highest order derivative terms. In addition, the load dependency of this type of friction generally causes the equations to be implicit in the joint accelerations. For the important case of load-dependent transmission friction, the equations are shown to be explicit. Techniques for the forward solution are described through the example of a roller screw transmission. Experimental and simulation results are used to show the importance of load-dependent friction in a particular robot. Implementational issues are discussed as well as implications for robot control.

1 Introduction

While commonly neglected because it is difficult to model and poorly understood, friction is present to some degree in all mechanical systems. Prior to the development of efficient formulations of the rigid-body dynamic equations such as the recursive Newton-Euler technique, robot controllers were (and in many cases still are) based on joint by joint PD control. This simple scheme degrades tracking performance at low and high velocities and places limits on the payload mass as well.

The inclusion of rigid-body dynamics in model-based control improves performance significantly. However, friction continues to impose limits on performance. The discontinuous nature of Coulomb-type friction near zero velocity causes stick-slip behavior which limits the fidelity of position and force control. As performance criteria, such as cycle time, are made more stringent and payload-to-arm mass ratios increase, the dynamic load dependency of friction becomes more important.

Though the constraints imposed by friction may be impossible to eliminate, a better understanding of friction phenomena is crucial to understanding and improving robot performance. Incorporating friction models into robot dynamic simulation provides a means to study these issues.

This paper examines the issues involved in including friction in the forward solution of the dynamic equations. Section 2 discusses the difficulty of modeling friction. In Section 3, the discontinuous and implicit nature of the frictional dynamic equations is described. Simple examples are used to illuminate these concepts. The special case of load-dependent friction in transmission

elements is discussed in Section 4. The explicitness of transmission friction is presented in the context of a screw drive. The scalar equations for raising and lowering a mass are included. In Section 5, the vector form of the forward dynamic equations with screw friction is presented. The importance of load-dependent friction is considered through the example of the roller screw transmissions in a particular robot. Section 6 describes the effect of combining transmission friction with other sources of friction at a joint. Section 7 presents conclusions and implications for robot control.

2 Friction Modeling

Friction is present in power transmission elements such as gears and screws as well as in bearings, seals, hydraulic components and electric motors. Friction behavior in each of these is a complex phenomenon. For example, friction in rolling-element bearings is a function of bearing size, type and design. Additional factors include speed, load type and magnitude as well as lubricant viscosity and flow [13]. While friction can be a function of many variables, it has been shown to be highly repeatable [2,3]. Thus friction modeling and parameter identification are viable goals.

Some researchers and manufacturers have developed theoretical or empirical friction models as well as typical values of the model parameters [9,11]. These parameter values provide only rough estimates of the behavior in a particular system. While it may be possible to use them to identify the dominant sources of friction in a system, the actual parameter values should be identified by experiment.

Due to the complexity of friction models in individual components, robotics researchers typically consider an aggregate friction model for each robot joint. This can be as simple as the kinetic / static friction model shown in Figure 1(a) or as detailed as that shown in Figure 1(b).
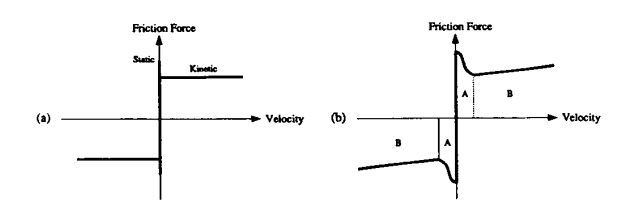

Figure 1: Friction Force Versus Velocity. (a) Kinetic / Static Model. (b) Complex Model.

The limited experimental modeling work in the literature describes two frictional effects near zero velocity. For extremely small displacements, elastic and plastic deformation at the friction interface generate a hysteresis effect [5]. Outside of this region, friction decreases with increasing velocity (region A in Figure 1(b)). The negative slope makes stable control in this region difficult, if not impossible. For moderate velocities, friction is reported to increase smoothly with velocity. In this region, labeled B in Figure 1(b), friction can be thought of as a combination of Coulomb and viscous friction.

By considering the standard Coulomb friction equation below, we can gain insight into the computational issues of robot friction simulation. Independent of the area of contact, the Coulomb friction force always opposes relative motion and is proportional to the normal force of contact [1]. This force can be expressed as

$$F_{friction} = \mu |F_N| sgn(velocity) \qquad (1)$$

where μ is the coefficient of friction and F_N is the normal force. The sign operator is defined as

$$sgn(x) = \begin{cases} +1 & , \quad x > 0 \\ 0 & , \quad x = 0 \\ -1 & , \quad x < 0 \end{cases} \qquad (2)$$

Due to its dependence on the sign of velocity, the friction force is discontinuous at zero velocity. In addition, the normal forces in robot components vary with joint positions, velocities and accelerations. This indicates that the governing differential equations are discontinuous in the highest order derivative terms.

In robot systems, the significance of friction normal-force dependence on joint positions, velocities and accelerations has not been thoroughly studied. Our analysis indicates that it is important in transmission elements. Its importance in bearing friction is unclear. If present, it will most likely be apparent for heavy payloads or at high velocities and accelerations when dynamic loading is greatest.

3 Robot Dynamics with Friction

The rigid-body dynamic equation including friction for an open-kinematic-chain robot is of the form

$$r = D(q)\ddot{q} + h(q,\dot{q}) + f(q,\dot{q},\ddot{q}) \qquad (3)$$

The vectors of joint displacements and actuator torques are q and r, respectively. Their dimension equals the number of degrees of freedom of the robot. The configuration-dependent inertia matrix is denoted by D. It is both symmetric and positive definite. The vector h consists of centrifugal, Coriolis and gravity terms. The vector f includes all friction terms and is a function of joint positions, velocities and accelerations.

The *inverse dynamics problem* is to solve for the joint torques or forces given the joint positions, velocities and accelerations. Efficient solution of this problem is necessary for model-based control. Regardless of the friction model used, inclusion of the frictional term does not substantially increase the difficulty of the problem if the Newton-Euler recursive equations are employed. In this method, the velocities and accelerations of the links are successively computed from the base outward. Using these quantities, the forces and moments at the joints are computed from the distal link inward. Consequently, the reaction forces and moments are readily available for use in computing the frictional torques.

The *forward dynamics problem* is to solve for the joint positions, velocities and accelerations given the input torques or forces and the initial conditions. This is the problem to be solved for robot
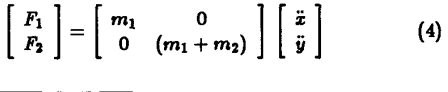
simulation. At each time step, the known joint torques, positions and velocities are used to compute the joint accelerations. In the absence of friction, this involves solving a set of linear algebraic equations. Given the special properties of the mass matrix, this can be done efficiently such as by using the Cholesky decomposition method [8]. Using the values of acceleration and velocity, numerical integration yields the velocity and position at the next time step.
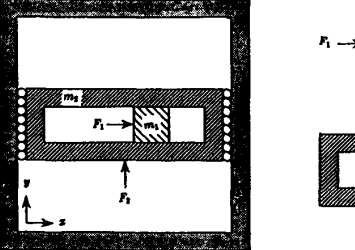
Friction increases the difficulty of the forward dynamic problem. Since the forces between the links vary with the positions, velocities and accelerations of all the joints, Coulomb-type friction can cause the governing differential equations to be both discontinuous and implicit in the highest order derivative terms.

3.1 Discontinuities in the Forward Solution

Let us investigate the discontinuity of the highest order derivatives by considering the X-Y Positioning System pictured in Figure 2. Mass 1 moves in the x-direction within the slot in Mass 2. Mass 2 moves in the y-direction within the square frame. The forces F_1 and F_2 are applied to the masses as shown. For clarity, gravity is not included in this analysis. First consider the frictionless case. Summing forces in the x and y directions, one can obtain the dynamic equations as shown below.

Mass 1: $\quad \sum F_x = m_1\ddot{x} = F_1$
$\qquad\qquad \sum F_y = m_1\ddot{y} = F_N$

Mass 2: $\quad \sum F_y = m_2\ddot{y} = F_2 - F_N$
$\qquad\qquad\qquad\quad\ = F_2 - m_1\ddot{y}$

$$\begin{bmatrix} F_1 \\ F_2 \end{bmatrix} = \begin{bmatrix} m_1 & 0 \\ 0 & (m_1+m_2) \end{bmatrix} \begin{bmatrix} \ddot{x} \\ \ddot{y} \end{bmatrix} \qquad (4)$$
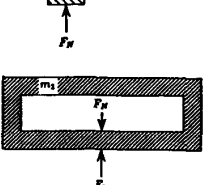

Figure 2: X-Y Positioning System.

Now let us include a Coulomb-friction force between masses 1 and 2 dependent on the normal force of contact. We can express this force as

$$F_{friction} = \mu |F_N| sgn(\dot{x}) \qquad (5)$$

The discontinuity in this expression is due to the term $sgn(\dot{x})$. (The absolute value operator causes a discontinuity in the derivative of $F_{friction}$.)

With friction, the dynamic equations become:

Mass 1: $\quad \sum F_x = m_1\ddot{x} = F_1 - \mu m_1 sgn(\dot{x})|\ddot{y}|$

$$\begin{bmatrix} F_1 \\ F_2 \end{bmatrix} = \begin{bmatrix} m_1 & 0 \\ 0 & (m_1+m_2) \end{bmatrix} \begin{bmatrix} \ddot{x} \\ \ddot{y} \end{bmatrix} + \begin{bmatrix} \mu m_1 \ddot{y} sgn(\dot{x}) sgn(F_2) \\ 0 \end{bmatrix} \qquad (6)$$

Notice that the frictional discontinuities do indeed occur in the

highest order derivative (acceleration) terms. In addition to $sgn(\dot{x})$, the equation also depends on $sgn(\ddot{y})$. In this case, however, $sgn(F_2) = sgn(\ddot{y})$. For this reason and because the direction of F_N is fixed in a local coordinate frame attached to Mass 2 (as explained in Section 3.2), Equation 6 is explicit in the accelerations.

As an illustration of the discontinuity and load dependence of Coulomb friction, the behavior of Mass 1 has been simulated using the parameter values listed below.

$$m_1 = 10 \quad F_1 = 8\sin(2.4t) \quad \mu = 0.3$$
$$m_2 = 30 \quad F_2 = 50\cos(0.8t)$$

Figures 3(a) and 3(b) are simulation plots showing the time history of Mass 1 without and with friction, respectively. Figure 3(b) contains an additional plot labeled *F-friction*. This quantity equals the magnitude of the friction force:

$$F\text{-}friction = \mu m_1 |\ddot{y}| \tag{7}$$

Comparing the acceleration curves in Figures 3(a) and 3(b), notice that the discontinuities in the frictional case occur when the velocity changes sign. The magnitude of the acceleration always decreases across a discontinuity. Also note that the magnitude of a discontinuity corresponds to the magnitude of *F-friction* at that point. At the velocity zero crossings close to $t = 2$ and $t = 6$, *F-friction* is near zero and the corresponding discontinuities in acceleration are small.

Friction also affects the overall magnitude of the acceleration curve. When the velocity and acceleration are of the same sign, friction is acting against the applied force and the magnitude of the acceleration is smaller with friction than without it. When the velocity and acceleration are of opposite sign, friction is acting in the same direction as the applied force and the acceleration with friction is of greater magnitude. Differences between the corresponding velocity and position curves are also apparent.

When integrating discontinuous ordinary differential equations, care must be taken to use the correct value of the derivative on each side of a discontinuity. Unfortunately, discontinuities generally occur inside an integration subinterval. The standard solution is to employ switching functions which flag the presence of a discontinuity (such as a velocity zero crossing) in the last
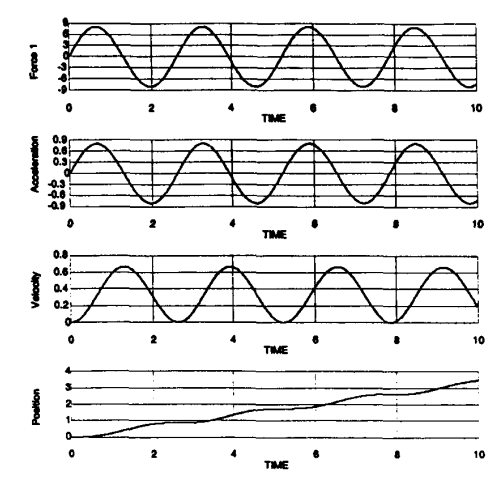

Figure 3: (a) Simulated Time History of Mass 1 Without Friction. Position measured relative to a local frame centered in Mass 2.
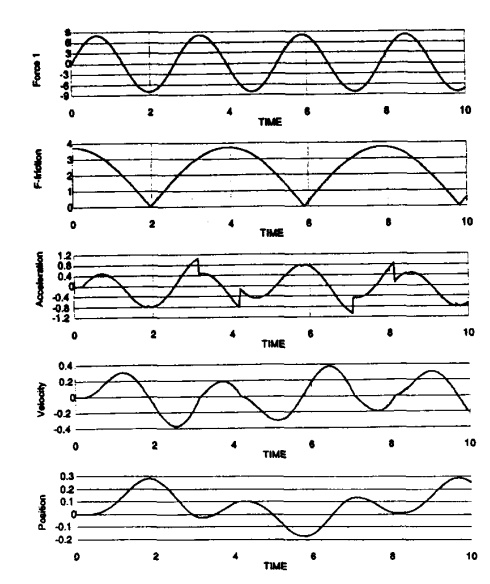

Figure 3: (b) Simulated Time History of Mass 1 With Friction. Position measured relative to a local frame centered in Mass 2.

subinterval. The integrator then backs up and searches for the switching time to within a specified tolerance. Integration up to the switching time is then repeated. The integration routine is then restarted from the discontinuity using the appropriate derivative value. Initially, small steps should be taken to accurately capture any transients which follow the discontinuity. If the friction model includes *stiction* (static friction), the integrator must also include tests for capture (sticking) and escape (break-away). These are discussed in Section 4.1.

Variable-step-size, variable-order methods are appropriate for integrating discontinuous equations. The plots appearing in Figure 3 were obtained using a method of this type. For synchronization purposes in real-time simulation and control, however, Morgowicz suggests the use of fixed-step-size methods [10]. By choosing the controller period as a multiple of the fixed step-size, the simulated robot state is available at controller sampling times. Discontinuities occurring during the previous subinterval are located using linear interpolation. Approximate values of the state derivatives on both sides of the discontinuity are computed. They are used to reintegrate the subinterval in one step.

3.2 Implicitness in the Forward Solution

In general, the inclusion of Coulomb or static friction in the robot dynamic equations renders them implicit in the joint accelerations. The forward solution requires an iterative root-finding process (such as a modified Newton method) at each step of the integration to compute the accelerations. A hybrid-computer alternative to iteration is described in [6].

The cause of the implicitness is the dependence of friction on the *magnitude* of the normal force. The normal force itself is a function of the resultant force and moment at the joint. Expressed in a local coordinate frame, the components of the resultant force and moment can be formulated in terms of the joint positions, velocities and accelerations. Just as with the net input forces or torques ($\tau - f$ in Equation 3), these components will be affine transformations of the accelerations.

If the direction of the normal force happens to be constant in the local frame, the normal force can be expressed as a function in which the net force and moment components appear linearly. This is true for friction in translational joints such as the X-Y Positioning System described in the previous section and for axially-loaded bearings when the axial load can be considered independently of radial load. Since the sign of the normal force can change, an absolute value operator must be used to obtain its magnitude.

When the direction of the normal force is not constant in a local joint coordinate frame, the magnitude of the normal force will involve the square root of sums of squares of net force and moment components. As an example, consider a radially-loaded joint bearing. The load can take on any direction between zero and 2π radians. In the planar case, for a local frame attached to the bearing with z as the bearing axis, the magnitude of the normal force is

$$F_{normal} = \sqrt{F_z^2 + F_y^2} \qquad (8)$$

where F_z and F_y are the x and y components of the bearing reaction force. In three dimensions, there are multiple bearings at a joint and one must consider joint geometry and reaction torques as well as reaction forces [7].

We see from the preceding paragraphs that Coulomb friction involves the absolute value or square root of sums of squares of acceleration-dependent terms. Substituting either type of expression into the original dynamic equation destroys its affine properties rendering it implicit in the accelerations. Consequently, it is necessary to iteratively solve for joint accelerations at each time step of a simulation.

For this reason, simulation of load-dependent friction terms appears to have a very high cost. This is not necessarily the case. For small friction coefficients, the zero-friction accelerations can be used to start the iterative process. Even better, Morgowicz [10] claims convergence in two iterations using as initial values the normal force magnitudes from the preceding time step. The cost of implicitness is significant, however. Using two iterations effectively requires two forward solutions in addition to solving the inverse problem once for those force and torque components needed to compute the normal forces.

For those cases when the magnitude involves only an absolute value operator, it can be possible to avoid an iterative solution. The absolute value operator could be replaced by a sign operator and incorporated in a switching function. This technique is used in the discussion of transmission friction which follows.

4 Friction in Transmission Elements

Transmission components such as gears, screws and harmonic drives are often used to convert high-speed, low-torque motor output to low-speed, high-torque joint motion. In these devices, not only is the direction of the frictional normal force fixed in the local coordinate frame, but the force can be represented by a function in which the input torque, output torque and rotor-inertia torque appear linearly. These torques are all present in the frictionless dynamic equations. Thus, no additional force or moment components need be computed.

A direct relationship exists between the effective input torque and the output torque (or force) which can be represented as an efficiency. The expression for the efficiency can replace the friction torque in the dynamic equations. Consequently, if we track the sign of the normal force with a switching function, transmission friction does not affect the explicitness of the forward dynamic equations. In the following sections, the nature of these equations is examined in the context of a screw drive.

4.1 Screw Friction

Screws are used to convert angular motion into linear motion. Typically, the screw rotates with the motor. The load is attached to the nut which translates as the screw rotates. The losses in a screw transmission are due to the rubbing between the screw and nut threads. A force analysis of the screw and nut can be found in many mechanical design texts such as [12]. While the output is a force, F_{out}, an output torque can be computed as the product

$$\tau_{out} = l \, F_{out} \qquad (9)$$

where the screw lead, l, is defined here as the distance the nut advances as the screw rotates through one radian. The efficiency is the ratio of output to input torques. It is a function of thread geometry and the coefficient of friction between the screw and nut.

Before discussing screws in the context of robot dynamics, consider the simple system in Figure 4 for raising and lowering a mass, m. Summing torques on the screw, we have

$$\tau_a = J_{zz}\ddot{q} + \tau_l + \tau_f \qquad (10)$$

The term, τ_a, is the applied motor torque. The terms on the right side of this equation correspond to the screw inertial torque, the load (output) torque and the friction torque. The displacement of the screw is given by q. The screw lead, l, relates the linear displacement of the mass, y, with q. The load torque is comprised of inertial and gravity components and is given by
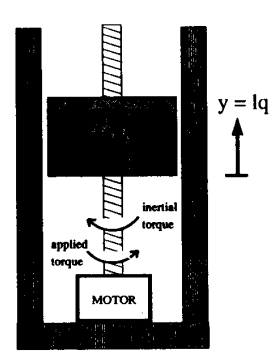
$$\tau_l = (ml\ddot{q} + mg)l \qquad (11)$$

Figure 4: Screw Drive for Positioning Mass, "m".

The friction torque, τ_f, can be eliminated from the torque equation by introducing the efficiency, η.

$$\eta = \frac{\tau_l}{\tau_{in}} \qquad (12)$$

$$\tau_{in} = \tau_a - J_{zz}\ddot{q} \qquad (13)$$

There are two expressions of efficiency, η_1 and η_2, for the cases of driving and backdriving the screw. These correspond to friction acting against and with τ_{in}, respectively. In the constant velocity case, they also correspond to raising and lowering the load.

$$\eta = \begin{cases} \eta_1 < 1, & sgn(\tau_l) = sgn(\dot{y}), \quad \text{Driving} \\ \\ \eta_2 > 1, & sgn(\tau_l) = -sgn(\dot{y}), \quad \text{Backdriving} \end{cases} \qquad (14)$$

Using the screw efficiency, the torque equation reduces to

$$\eta(\tau_a - J_{zz}\ddot{q}) = \tau_l \qquad (15)$$

1373

Selection of the appropriate value of η requires the signs of both the velocity and load torque. The sign of the load torque corresponds to the sign of the normal force of friction. The velocity and load torque must be included in the switching function used to integrate this equation. A velocity zero crossing would indicate the presence of a discontinuity in $\ddot{q}$ during the preceding integration subinterval. A load-torque zero crossing indicates a change in the slope of $\ddot{q}$. Note that friction models expressing η as a function of such variables as position and velocity would not affect the solution procedure.

Notice how the screw inertial torque is not included as part of the load torque in Equation 15. Motor rotor inertia should be treated in the same way. Since J_{ss} is typically small compared to the load torque, it is reasonable to question the importance of isolating it from the load torque. However, note that the screw lead, l, amplifies the rotational screw inertia by the factor $1/l^2$.

The system in Figure 4 was simulated with the following parameter values chosen to clearly illustrate the dependence of acceleration on the signs of both velocity and load torque.

$$ml^2 = 50 \quad \tau_{in} = 750\sin(4t)$$
$$J_{ss} = 5 \quad g = 0$$
$$\eta_1 = .663 \quad \eta_2 = 1.91$$

The simulation plots appear in Figure 5. The discontinuities in the acceleration, $\ddot{q}$, at velocity zero crossings are apparent. In addition, a change in the slope of $\ddot{q}$ occurs at load torque zero crossings. Since gravity was taken to be zero, the load torque and the acceleration pass through zero simultaneously. One might suspect that if this were not the case, load-torque zero crossings would also cause discontinuities. However, examination of the equations shows that, irrespective of the value of g, zero crossings of τ_l cause discontinuities in jerk, $\dddot{q}$, but not in acceleration.

Up to this point, friction at zero velocity has been neglected. Equation 15 is really only valid for nonzero velocities. A simple static friction model will be used to outline the forward dynamic solution of sticking joints.

At zero velocity, the static friction force assumes the magnitude and direction necessary to prevent motion. Its maximum magnitude is at least the Coulomb value and is generally higher. Static values of the efficiences can be computed using static friction coefficients.

$$\eta_{1s} \leq \eta_1 < 1 \tag{16}$$

$$\eta_{2s} \geq \eta_2 > 1$$

Consider when the screw is stuck due to friction. Both $\dot{q}$ and $\ddot{q}$ are zero. For the given value of load torque ($\tau_l = mgl$), there exists a band of applied torques for which no motion will ensue. This deadband is defined by the inequalities

$$\tau_l/\eta_{2s} \leq \tau_a \leq \tau_l/\eta_{1s}, \quad \tau_l > 0$$
$$\tau_l/\eta_{1s} \leq \tau_a \leq \tau_l/\eta_{2s}, \quad \tau_l < 0 \tag{17}$$

and is pictured on the ordinate axis in Figure 6 for $\tau_l > 0$. Escape from static friction (break-away) will occur when τ_a moves outside of this deadband. The direction of motion is determined by which inequality is violated. The screws used in robotic applications are not self-locking. This means that if the applied torque in Figure 4 is zero, the mass will descend under the force of gravity.

So far, we have described the case when the screw is initially at rest. There is actually a second case when static friction must be considered. This occurs when the velocity is initially nonzero and changes sign during an integration subinterval. There are two possible discontinuities in acceleration at the zero crossing. In one, stiction occurs forcing $\dot{q}$ and $\ddot{q}$ to zero. In the other, no
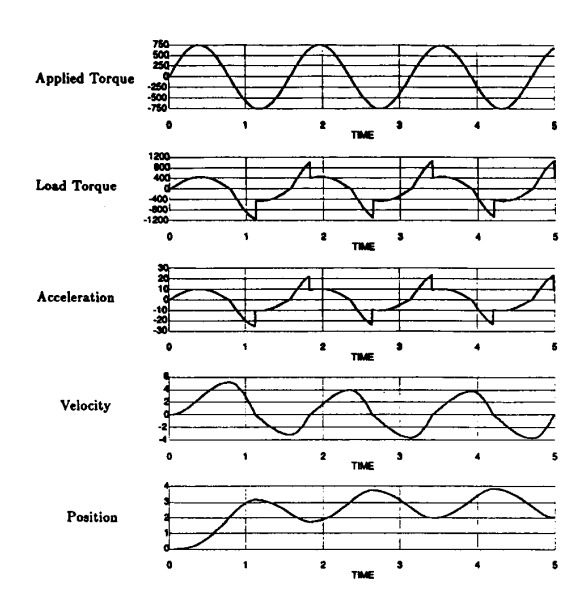

Figure 5: Simulated Time History of the Screw. Position, velocity and acceleration refer to q, $\dot{q}$ and $\ddot{q}$, respectively.
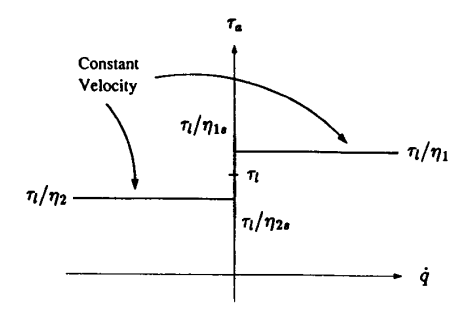

Figure 6: Screw Applied Torque versus Velocity Plot Showing Stiction Deadband for $\tau_l > 0$.

stiction occurs, but rather the velocity changes sign. To determine which discontinuity occurs, the stiction inequality is evaluated at the time of the velocity zero crossing with $\ddot{q}$ assumed to be zero. If the applied torque at that instant falls outside the stiction deadband then the value of η changes, but stiction does not occur.

In actuality, the friction model used in the preceding simulation included static friction. Stiction did not occur for two reasons. With $g = 0$, τ_l is zero at break-away ($t = 0$) and so no friction force can be generated. Secondly, the magnitude and frequency of τ_a are high enough that it is always outside the stiction deadband at velocity zero crossings.

5 Screw Friction in the Robot Forward Dynamic Equation

One example of a robot which uses screw drives is the Field Materiel Handling Robot (FMR) pictured in Figure 7. Currently under construction by Martin Marietta Aero and Naval Systems for the US Army, the FMR is designed for palletized supply handling.

$$
\begin{bmatrix}
d_{11} & \cdots & & \cdots & & \cdots & \cdots & d_{1n} \\
\vdots & & & & & & & \vdots \\
d_{i-1,1} & & & & & & & d_{i-1,n} \\
d_{i1} + (\eta - 1)a_{i1} & \cdots & d_{ii} + (\eta - 1)a_{ii} & d_{i,i+1} & \cdots & & & d_{in} \\
d_{i+1,1} & & & & & & & d_{i+1,n} \\
\vdots & & & & & & & \vdots \\
d_{n1} & \cdots & & \cdots & & \cdots & \cdots & d_{nn}
\end{bmatrix} \ddot{q}
$$

$$
+ \begin{bmatrix}
h_1 \\
\vdots \\
h_{i-1} \\
h_i + (\eta - 1)b_i \\
h_{i+1} \\
\vdots \\
h_n
\end{bmatrix} = \begin{bmatrix}
\tau_1 \\
\vdots \\
\tau_{i-1} \\
\eta \tau_i \\
\tau_{i+1} \\
\vdots \\
\tau_n
\end{bmatrix} \qquad (22)
$$

which is explicit in $\ddot{q}$. Thus for a screw in motion, the form of the dynamic equations is reduced to that of the frictionless case.

Now we will consider the static case. Recall that when a screw is sticking, $\dot{q}_{screw} = \ddot{q}_{screw} = 0$. To determine if break-away occurs, the same inequalities as the scalar case are employed.

$$
\tau_i^l / \eta_{2s} \leq \tau_i \leq \tau_i^l / \eta_{1s}, \quad \tau_i^l > 0
$$
$$
\tau_i^l / \eta_{1s} \leq \tau_i \leq \tau_i^l / \eta_{2s}, \quad \tau_i^l < 0 \qquad (23)
$$

In this case the load torque on screw i is given by

$$
\tau_i^l = \sum_{j=1}^{n} d_{ij} \ddot{q}_j + h_i - \tau_i^s \qquad (24)
$$

The screw inertial torque in the equation above is not necessarily zero due to contributions from the motion of preceding links. The accelerations of the other joints are needed to solve for τ_i^l. They can be computed using the explicit equation

$$
\begin{bmatrix}
d_{11} & \cdots & d_{1,i-1} & d_{1i} & d_{1,i+1} & \cdots & d_{1n} \\
\vdots & & & & & & \vdots \\
d_{i-1,1} & & & & & & d_{i-1,n} \\
0 & \cdots & 0 & 1 & 0 & \cdots & 0 \\
d_{i+1,1} & & & & & & d_{i+1,n} \\
\vdots & & & & & & \vdots \\
d_{n1} & \cdots & d_{n,i-1} & d_{ni} & d_{n,i+1} & \cdots & d_{nn}
\end{bmatrix} \ddot{q} + \begin{bmatrix}
H_1 \\
\vdots \\
H_{i-1} \\
0 \\
H_{i+1} \\
\vdots \\
H_n
\end{bmatrix}
$$

$$
= \begin{bmatrix}
\tau_1 \\
\vdots \\
\tau_{i-1} \\
0 \\
\tau_{i+1} \\
\vdots \\
\tau_n
\end{bmatrix} \qquad (25)
$$

To enforce $\ddot{q}_{screw} = 0$, the ith rows of τ, D and h (associated with the sticking screw joint) are set to zero except for the ii^{th} element of D which is set to one.

Through systematic application of the preceding equations, the friction in any number of screw joints can be included. To solve for the accelerations, each row of the dynamic equation corresponding to a screw joint is modified according to either Equation 28 or 31. The dynamic equations remain affine transformations of the joint accelerations. The load torque can then be computed for each screw joint using Equation 30. These values can be used to test for break-away of sticking joints and in the switching functions used to select η_i for screws in motion. Similar equations can be derived for other transmission elements.
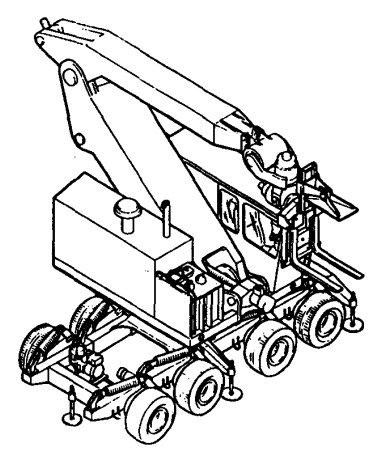

Figure 7: The Field Materiel Handling Robot. Roller screws are used to drive the shoulder and elbow joints.

This hydraulically-driven, six degree-of-freedom robot possesses a 25-foot reach and 2-ton payload capacity. Due to stringent cycle time and transportability requirements, friction and flexure represent two potential challenges to the controller.

Roller screws are used to actuate the shoulder and elbow joints. Along with the hydraulic components, they are expected to be the dominant frictional elements. Roller screws differ from ordinary screws in that they include planetary, threaded rollers between the screw and the nut. The rollers substitute rolling and spinning friction for the much larger rubbing friction which occurs between the simple screw and nut. Friction remains significant, however.

While not available in the literature, theoretical friction models have been developed by roller screw manufacturers. These models are complex, highly application dependent and proprietary [9]. In their place, the manufacturer provides the customer with theoretical parameter values for the friction angle factor, K, the nominal diameter, d, and the screw lead, l, to be used in the efficiency equations for ordinary power screws which are given below.

$$
\eta_1 = \left(1 + \frac{Kd}{l}\right)^{-1} \qquad \eta_2 = \left(1 - \frac{Kd}{l}\right)^{-1} \qquad (18)
$$

Consider first the case when the screw at joint i is moving.

$$
\eta(\tau_i - \tau_i^s) = \sum_{j=1}^{n} d_{ij} \ddot{q}_j + h_i - \tau_i^s \qquad (19)
$$

In this equation, τ^s represents the screw inertial torque seen by the motor. Since the equations for D and h include the screw inertia, it is explicitly subtracted from the right side of the equation.

By examining the Newton-Euler recursive equations, the screw inertial torque about the screw axis is found to be the z component of N_s where

$$
N_s = I_s \dot{\omega}_s + \omega_s \times (I_s \omega_s) \qquad (20)
$$

The inertia tensor of the screw is I_s and ω_s is the screw's angular velocity. Both are expressed in a local coordinate frame attached to the screw. Furthermore, the second term in N_s does not contribute since, for the screw, $I_{zz} = I_{yy}$. The vector $\dot{\omega}_s$ is a function of the velocities and accelerations of the screw joint and all preceding joints. The general form of τ^s for a screw at joint i is

$$
\tau_i^s = [a_{i1}(q), \ldots, a_{ii}(q), 0, \ldots, 0] \ddot{q} + b_i(q, \dot{q}) \qquad (21)
$$

Substituting this equation into the system of equations we have

In the FMR, the theoretical value of η_1 lies in the range of 0.8 to 0.9. Experimental data confirms that friction at the shoulder and elbow joints is dominated by screw friction. The total friction torque at these joints is proportional to the load torque. The actual value of η_1 is between 0.6 and 0.7 indicating about a third of the motor torque is consumed by friction during driving. The static efficiency may be up to 25% lower [9]. Simulations indicate that the shoulder-screw load torque (and thus, friction torque) can vary dynamically by $\pm 23\%$ from its average value during an unloaded trajectory. Of course, a comparison of loaded and unloaded trajectories would show an even greater variation in transmission friction. Simulations also show that the screw inertial torque at the elbow can be over 9% of τ_l during smooth trajectory segments and over 25% during transients.

6 Combining Friction Terms

When the friction model for a particular joint includes more than transmission friction, the dynamic equations can take on one of two possible forms. Denoting the motor torque by τ_m, the screw load torque by τ_l and the additional friction torque by τ_f, the two equations are

$$\tau_m = \tau_s + (1 \pm k)\tau_l + \tau_f \tag{26}$$
$$\tau_m = \tau_s + (1 \pm k)(\tau_l + \tau_f) \tag{27}$$

The term τ_s corresponds to screw and possibly motor rotor inertial torque. The reciprocal of efficiency is represented by $(1 \pm k) > 0$. The signs apply to driving and backdriving the screw, respectively.

Equation 32 applies when the additional friction does not contribute to the load torque. This is true of any friction which must be overcome to spin the screw even when the nut is removed. In the FMR, this would be true of friction in the screw motors.

Equation 33 applies when the additional friction contributes to the transmission load torque. This would apply to friction in the bearings of the three pivot joints forming a closed kinematic chain in the FMR. In this case, when the motor is driving the joint, transmission friction has the effect of amplifying the other friction losses. During backdriving, the braking effect of the additional friction term is attenuated by transmission friction.

The value of k could be as high as 0.5 ($\eta_1 = 0.667$). Use of the wrong equation could result in significant simulation errors. When friction parameters are identified experimentally, these equations can explain unexpected directional asymmetries in the friction. The amplification effect could also increase the importance of a marginal friction contributor necessitating its inclusion in the friction model.

7 Conclusions

Increasingly stringent performance constraints and higher payload to arm mass ratios make accurate robot modeling important for both simulation and control. In this paper, the effect of friction on the solution of the forward dynamics problem was examined. Two factors were identified as making the problem more difficult than the frictionless case. The differential equations are discontinuous in the highest order derivative terms (accelerations) and, for load-dependent friction, implicit in the general case. Transmission friction was shown to be one form of load-dependent friction for which the equations are explicit. This was described in the context of screw drives for which the robot forward dynamic equations with static and Coulomb friction were developed.

7.1 Implications for Control

Friction parameters vary with load as well as with many environmental factors. Model-based, adaptive control has been proposed by researchers as a way of coping with the variations [4]. This is a good approach, but should be used with friction models whose structure is chosen according to the behavior of the predominant friction contributors in a particular robot. The necessary model detail will be determined by the performance requirements of the robot.

It is not necessarily correct to use a simple aggregate friction model at each joint. Analysis has shown, for example, that the load dependency of screw friction in the FMR cannot be neglected. In some cases, load-dependency, such as in bearing friction, may be unimportant. With further study, it may be possible to identify general friction models for different types of robots. Simulation combined with experiment can be used to develop these models as well as to refine them for a particular system.

Acknowledgement

8 References

1. A. W. Adamson, *Physical Chemistry of Surfaces.* 4th edition, John Wiley & Sons, New York, 1982.

2. B. Armstrong, "Dynamics for Robot Control: Friction Modeling and Ensuring Excitation During Parameter Identification." Ph.D. Dissertation, Electrical Engineering, Stanford University, May 1988, Report No. STAN-CS-88-1205.

3. B. Armstrong, "Friction: Experimental Determination, Modeling and Compensation." *Proceedings 1988 IEEE Int. Robotics and Automation Conf.*, Philadelphia, PA, April, 1988.

4. C. Canudas De Wit, P. Noel et al, "Adaptive Friction Compensation in Robot Manipulators: Low-Velocities." *Proceedings 1989 IEEE Int. Robotics and Automation Conf.*, Scottsdale, April, 1989.

5. P.R. Dahl, "Measurement of Solid Friction Parameters of Ball Bearings." *Proc. of 6th Annual Symp. on Incremental Motion Control Systems and Devices*, University of Illinois, 1977.

6. A. Gogoussis and M. Donath, "Modeling robots: A Real Time Method for Solving the Forward Dynamics Problem Incorporating Friction." *Proceedings of the US - Japan Symposium on Flexible Automation*, ASME, Minneapolis, MN, 1988.

7. A. Gogoussis and M. Donath, "Coulomb Friction Effects on the Dynamics of Bearings and Transmissions in Precision Robot Mechanisms." *Proceedings 1988 IEEE Int. Robotics and Automation Conf.*, Philadelphia, PA, April, 1988.

8. D. Jacobs, *The State of the Art in Numerical Analysis.* Academic Press, London, 1977.

9. P.C. Lemor, SKF Component Systems Corporation, Bethlehem, PA, Personal Communication, October, 1989.

10. B. Morgowics, "Techniques for Real-time Simulation of Robot Manipulators." Ph.D. Dissertation, Aerospace Engineering, University of Michigan, 1988.

11. A. Palmgren, *Ball and Roller Bearing Engineering.* S.H. Burbank and Co., Philadelphia, 1945.

12. J.E. Shigley, *Mechanical Engineering Design.* 3^d Edition, McGraw-Hill Book Company, 1977.

13. A.Z. Sseri, *TRIBOLOGY Friction, Lubrication and Wear.* McGraw-Hill Book Company, New York, 1980.